T23
hep-ph/0105248

New Progress in Time-Like Exclusive Processes

Chueng-Ryong Ji
Department of Physics, North Carolina State University
Ho-Meoyng Choi
Department of Physics, Carnegie Mellon University

We discuss a necessary nonvalence contribution in timelike exclusive processes. Following a Schwinger-Dyson type of approach, we relate the nonvalence contribution to an ordinary light-front wave function that has been extensively tested in the spacelike exclusive processes. A complicate multi-body energy denominator is exactly cancelled in summing the light-front time-ordered amplitudes. Applying our method to $K_{\ell 3}$ and $D^0 \to K^- \ell^+ \nu_\ell$ where a rather substantial nonvalence contribution is expected, we find not only an improvement in comparing with the experimental data but also a covariance(that is, frame-independence) of existing light-front constituent quark model.

1. INTRODUCTION

As discussed in this PEP-N meeting, the facilities that copiously produce the lower-lying mesons such as K and D can provide a lot of rich physics as exciting as the new and upgraded B-meson factories promise. To fulfill such excitement, however, intensive theoretical studies should be accompanied in the analyses of exclusive meson decays and form factors. Thus, more and more scrutinized model analyses are called for.

Perhaps, one of the most popular formulations for the analysis of exclusive processes may be provided in the framework of light-front (LF) quantization [1]. In particular, the Drell-Yan-West ($q^+ = q^0 + q^3 = 0$) frame has been extensively used in the calculation of various electroweak form factors and decay processes [2–5]. As an example, only the parton-number-conserving (valence) Fock state contribution is needed in $q^+ = 0$ frame when the "good" component of the current, J^+ or $\mathbf{J}_\perp = (J_x, J_y)$, is used for the spacelike electromagnetic form factor calculation of pseudoscalar mesons. The LF approach may also provide a bridge between the two fundamentally different pictures of hadronic matter, i.e. the constituent quark model (CQM) (or the quark parton model) closely related to the experimental observations and the quantum chromodynamics (QCD) based on a covariant non-abelian quantum field theory. The crux of possible connection between the two pictures is the rational energy-momentum dispersion relation that leads to a relatively simple vacuum structure. There is no spontaneous creation of massive fermions in the LF quantized vacuum. Thus, one can immediately obtain a constituent-type picture, in which all partons in a hadronic state are connected directly to the hadron instead of being simply disconnected excitations (or vacuum fluctuations) in a complicated medium. A possible realization of chiral symmetry breaking in the LF vacuum has also been discussed in the literature [6].

On the other hand, the analysis of timelike exclusive processes (or timelike $q^2 > 0$ region of bound-state form factors) remained as a rather significant challenge in the LF approach. In principle, the $q^+ \neq 0$ frame can be used to compute the timelike processes but then it is inevitable to encounter the particle-number-nonconserving Fock state (or nonvalence) contribution. The main source of difficulty in CQM phenomenology is the lack of information on the non-wave-function vertex (black blob in Figure 1(a)) in the nonvalence diagram arising from the quark-antiquark pair creation/annihilation. The non-wave-function vertex (black blob) was recently also called the embedded state [7]. This should contrast with the white blob representing the usual LF valence wave function.

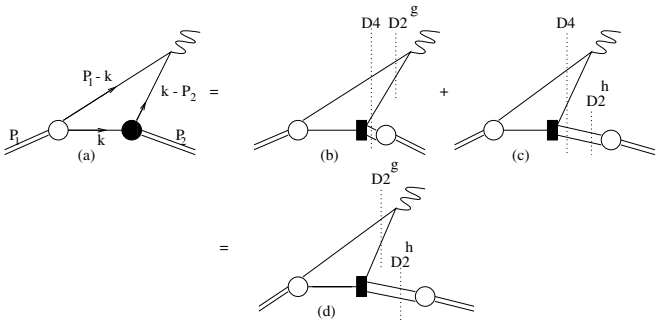

Figure 1: Effective treatment of the LF nonvalence amplitude.

In principle, there is a systematic program laid out by Brodsky and Hwang [8] to include the particle-number-nonconserving amplitude to take into account the nonvalence contributions. However, such a program requires to find all the higher Fock-state wave functions while there has been relatively little progress in computing the basic wave functions of hadrons from first principles. Recently, a method of analytic continuation from the spacelike region has also been suggested to generate necessary information in the timelike region without encountering a direct calculation of the nonvalence contribution [9]. Even though some explicit example

has been presented for manifestly covariant theoretical models, this method has not yet been implemented to more realistic phenomenological models.

In this talk, we thus present an alternative way of handling the nonvalence contribution. Our aim of new treatment [10] is to make the program more suitable for the CQM phenomenology specific to the low momentum transfer processes. Incidentally, the light-to-light ($K_{\ell 3}$) and heavy-to-light ($D^0 \to K^-\ell^+\nu_\ell$) decays involving rather low momentum transfers bear a substantial contribution from the nonvalence part and their experimental data are better known than other semileptonic processes with large momentum transfers. Including the nonvalence contribution, our results on $K_{\ell 3}$ and $D^0 \to K^-\ell^+\nu_\ell$ not only show a definite improvement in comparison with experimental data but also exhibit a covariance (that is, frame-independence) of our approach.

This talk is organized as follows. In Section 2, we present the non-wave-function vertex in the nonvalence diagram in terms of light-front vertex functions, utilizing the covariant Bethe-Salpeter(BS) model of (3+1)-dimensional fermion field theory. The nonvalence part of the weak form factors for $0^- \to 0^-$ semileptonic decays is expressed in terms of light-front vertex functions of a hadron and a gauge boson. The link operator connecting $(n-1)$-body to $(n+1)$-body in a Fock state representation is obtained by an analytic continuation of the usual BS amplitude. We also show that the complicated $(n+2)$-body energy denominators are exactly cancelled in summing the light-front time-ordered diagrams. In Section 3, we show our numerical results for $K_{\ell 3}$ and $D^0 \to K^-\ell^+\nu_\ell$ decays. Conclusions follow in Section 4.

2. NEW EFFECTIVE TREATMENT

2.1. $0^- \to 0^-$ Semileptonic Decays

The semileptonic decay of $Q_1\bar{q}$ bound state with four-momentum P_1^μ and mass M_1 into another $Q_2\bar{q}$ bound state with P_2^μ and M_2 is governed by the weak current, viz.,

$$\begin{aligned} J^\mu(0) &= \langle P_2|\bar{Q}_2\gamma^\mu Q_1|P_1\rangle \\ &= f_+(q^2)(P_1+P_2)^\mu + f_-(q^2)q^\mu, \end{aligned} \tag{1}$$

where $q^\mu = (P_1-P_2)^\mu$ is the four-momentum transfer to the lepton pair ($\ell\nu$) and $m_\ell^2 \le q^2 \le (M_1-M_2)^2$. The covariant three-point Bethe-Salpeter (BS) amplitude of the total current $J^\mu(0)$ in Eq. (1) may be given by

$$\begin{aligned} J^\mu(0) &= iN_c\int \frac{d^4k}{(2\pi)^4}\frac{H_1^{\rm cov}H_2^{\rm cov}S^\mu}{(p_1^2-m_1^2+i\varepsilon)(p_2^2-m_2^2+i\varepsilon)} \\ &\quad\times\frac{1}{(p_{\bar{q}}^2-m_{\bar{q}}^2+i\varepsilon)}, \end{aligned} \tag{2}$$

where N_c is the color factor, $H_{1[2]}^{\rm cov}$ is the covariant intitial[final] state meson-quark vertex function that satisfies the BS equation, and $S^\mu = {\rm Tr}[\gamma_5(\not{p}_1+m_1)\gamma^\mu(\not{p}_2+m_2)\gamma_5(-\not{p}_{\bar{q}}+m_{\bar{q}})]$. The quark momentum variables are given by $p_1 = P_1-k$, $p_2 = P_2-k$, and $p_{\bar{q}} = k$.

As shown in the literature [7], the LF energy integration reveals an explicit correspondence between the sum of LF time-ordered amplitudes and the original covariant amplitude. For instance, performing the k^- pole integration, we obtain the LF currents, J_V^μ and J_{NV}^μ corresponding to the usual LF valence diagram and the nonvalence diagram shown in Figure 1(a), respectively. Since $H_2^{\rm cov}$ satisfies the BS equation, we iterate $H_2^{\rm cov}$ once and perform its LF energy integration to find the corresponding LF time-ordered diagrams Figures 1(b) and 1(c) after the iteration. The similar idea of iteration in a Schwinger-Dyson (SD) type of approach was presented in [11] to pin down the LF bound-state equation starting from the covariant BS equation.

Comparing the LF time-ordered expansions before and after the iteration, we realize that the following link between the non-wave-function vertex (black blob) and the ordinary LF wave function (white blob) as shown in Figure 2 naturally arises, that is,

$$\begin{aligned} &(M^2-\mathcal{M}_0^2)\Psi'(x_i,\mathbf{k}_{\perp i}) \\ &= \int [dy][d^2\mathbf{l}_\perp]\mathcal{K}(x_i,\mathbf{k}_{\perp i};y_j,\mathbf{l}_{\perp j})\Psi(y_j,\mathbf{l}_{\perp j}), \end{aligned} \tag{3}$$

where M is the mass of outgoing meson and $\mathcal{M}_0^2 = (m_1^2+\mathbf{k}_{\perp 1}^2)/x_1 - (m_2^2+\mathbf{k}_{\perp 2}^2)/(-x_2)$ with $x_1 = 1-x_2 > 1$ due to the kinematics of the non-wave-function vertex.

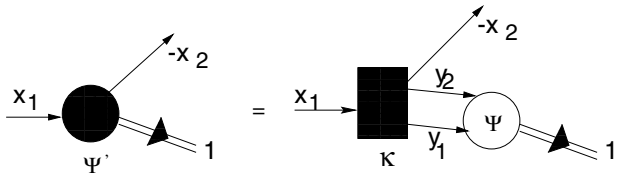

Figure 2: Non-wave-function vertex(black blob) linked to an ordinary LF wave function(white blob).

We note that Eq. (3) essentially takes the same form as the LF bound-state equation (similar to the LF projection of BS equation) except the difference in kinematics (for example, $-x_2 > 0$ for the non-wave-function vertex). Incidentally, Einhorn [12] also discussed the extension of the LF BS amplitude in 1 + 1 QCD to a non-wave-function vertex similar to what we obtained in this work.

In the above procedure, we also find that the four-body energy denominator D_4 is exactly cancelled in the sum of LF time-ordered amplitudes as shown in Figures 1(b) and 1(c), that is, $1/D_4D_2^g + 1/D_4D_2^h = 1/D_2^gD_2^h$. We thus obtain the amplitude identical to the nonvalence contribution in terms of ordinary LF wave functions of gauge boson (W) and hadron (white blob) as drawn in Figure 1(d). This method, however, requires to have some relevant operator depicted as the black square ($\mathcal{K}$) in Figure 2 (see also Figure 1(d)), that is in general dependent on the involved momenta connecting one-body to three-body sector. We now present some details of kinematics in the semileptonic decay processes to discuss a reasoning of how we handle the nonvalence contribution involving the momentum-dependent $\mathcal{K}$ for relatively small momentum transfer processes such as π_{e3}, $K_{\ell 3}$ and $D \to K\ell\nu$.

2.2. Kinematics and Model Description

Our calculation is performed in purely longitudinal momentum frame [10, 13] where $q^+ > 0$ and $\mathbf{P}_{1\perp} = \mathbf{P}_{2\perp} = 0$ so that the momentum transfer square $q^2 = q^+q^- > 0$ is time-like. One can then easily obtain q^2 in terms of the momentum fraction $\alpha = P_2^+/P_1^+ = 1-q^+/P_1^+$ as $q^2 = (1-\alpha)(M_1^2 - M_2^2/\alpha)$. Accordingly, the two solutions for α are given by

$$\alpha_\pm = \frac{M_2}{M_1}\left[\frac{M_1^2+M_2^2-q^2}{2M_1M_2} \pm \sqrt{\left(\frac{M_1^2+M_2^2-q^2}{2M_1M_2}\right)^2 - 1}\right]. \quad (4)$$

The $+(-)$ sign in Eq. (4) corresponds to the daughter meson recoiling in the positive (negative) z-direction relative to the parent meson. At zero recoil ($q^2 = q^2_{\max}$) and maximum recoil($q^2 = 0$), $\alpha_\pm$ are given by

$$\alpha_+(q^2_{\max}) = \alpha_-(q^2_{\max}) = \frac{M_2}{M_1},$$
$$\alpha_+(0) = 1, \qquad \alpha_-(0) = \left(\frac{M_2}{M_1}\right)^2. \quad (5)$$

In order to obtain the form factors $f_\pm(q^2)$ which are independent of $\alpha_\pm$, defining $J^+(0)|_{\alpha=\alpha_\pm} \equiv 2P_1^+H^+(\alpha_\pm)$ from Eq. (1), we obtain

$$f_\pm(q^2) = \pm\frac{(1\mp\alpha_-)H^+(\alpha_+) - (1\mp\alpha_+)H^+(\alpha_-)}{\alpha_+ - \alpha_-}. \quad (6)$$

The form factors $f_+(q^2)$ and $f_-(q^2)$ are related to the scalar form factor $f_0(q^2)$ in the following way:

$$f_+(0) = f_0(0), \quad f_0(q^2) = f_+(q^2) + \frac{q^2}{M_1^2 - M_2^2} f_-(q^2). \quad (7)$$

The differential decay rate for $0^- \to 0^-$ semileptonic decay is given by [4]

$$\frac{d\Gamma}{dq^2} = \frac{G_F^2}{24\pi^3}|V_{q_1\bar{q}_2}|^2 K_f(q^2)(1-\frac{m_l^2}{q^2})^2 \times \left\{[K_f(q^2)]^2\left(1+\frac{m_l^2}{2q^2}\right)|f_+(q^2)|^2 + M_1^2\left(1-\frac{M_2^2}{M_1^2}\right)^2\frac{3}{8}\frac{m_l^2}{q^2}|f_0(q^2)|^2\right\}, \quad (8)$$

where G_F is the Fermi constant, $V_{q_1\bar{q}_2}$ is the element of the Cabbibo-Kobayashi-Maskawa (CKM) mixing matrix and the factor $K_f(q^2)$ is given by

$$K_f(q^2) = \frac{1}{2M_1}\left[(M_1^2+M_2^2-q^2)^2 - 4M_1^2M_2^2\right]^{1/2}. \quad (9)$$

With the iteration procedure Eq. (3) in this $q^+ > 0$ frame, the results for the "+"-component of the current J^μ in Eq. (2) are given by

$$J_V^+ = \frac{N_c}{16\pi^3}\int_0^\alpha dx\int d^2\mathbf{k}_\perp \frac{\Psi_i(x,\mathbf{k}_\perp)S_V^+\Psi_f(x',\mathbf{k}_\perp)}{x(1-x)(1-x')}, \quad (10)$$

and

$$J_{NV}^+ = \frac{N_c}{16\pi^3}\int_\alpha^1 dx\int d^2\mathbf{k}_\perp \frac{\Psi_i(x,\mathbf{k}_\perp)S_{NV}^+}{x(1-x)(x'-1)}\Psi_g(x,\mathbf{k}_\perp) \times\int\frac{1}{y(1-y)}\int d^2\mathbf{l}_\perp\mathcal{K}(x,\mathbf{k}_\perp;y,\mathbf{l}_\perp)\Psi_f(y,\mathbf{l}_\perp), \quad (11)$$

where Eq. (3) has been used for the nonvalence wave function at the black blob as shown in Figure 2 (see also Figure 1(d)).

The ordinary LF vertex functions(white blob in Figure 1) in Eqs. (10) and (11) are given by

$$\Psi_i = \frac{h_1^{\rm LF}}{M_1^2 - M_{01}^2},\ M_{01}^2 = \frac{m_1^2+\mathbf{k}_\perp^2}{1-x} + \frac{m_{\bar{q}}^2+\mathbf{k}_\perp^2}{x},$$
$$\Psi_f = \frac{h_2^{\rm LF}}{M_2^2 - M_{02}^2},\ M_{02}^2 = \frac{m_2^2+\mathbf{k}_\perp^2}{1-x'} + \frac{m_{\bar{q}}^2+\mathbf{k}_\perp^2}{x'}, \quad (12)$$

where $x = k^+/P_1^+$, $x' = x/\alpha$. The Ψ_g in Eq. (11) corresponds to the light-front energy denominator (that is, D_g in Figure 1(d)) and its explicit form is given by

$$\Psi_g(x,\mathbf{k}_\perp) = \frac{1}{\alpha\left[\frac{q^2}{1-\alpha} - \left(\frac{\mathbf{k}_\perp^2+m_1^2}{1-x} + \frac{\mathbf{k}_\perp^2+m_2^2}{x-\alpha}\right)\right]}. \quad (13)$$

We call Ψ_g the light-front vertex function of a gauge boson[1].

In Eqs. (10) and (11), the trace terms $S_V^+(p_{\bar{q}}^- = k_{\rm on}^-) = (4P_1^+/x')\{\mathbf{k}_\perp^2 + [xm_1 + (1-x)m_{\bar{q}}][x'm_2 + (1-x')m_{\bar{q}}]\}$ and $S_{NV}^+(p_1^- = p_{1\rm on}^-) = S_V^+(p_i^- = p_{i\rm on}^-) + 4p_{1\rm on}^+p_{2\rm on}^+(p_{\bar{q}}^- - p_{\bar{q}\rm on}^-)$ correspond to the product of initial and final LF spin-orbit wave functions that are uniquely determined by a generalized off-energy-shell Melosh transformation. Here, the subscript (on) means on-mass-shell and the instantaneous part of nonvalence diagram corresponds to $4p_{1\rm on}^+p_{2\rm on}^+(p_{\bar{q}}^- - p_{\bar{q}\rm on}^-)$ in S_{NV}^+. While the LF vertex function $h_{1[2]}^{LF}$ formally stems from $H_{1[2]}^{\rm cov}$, practical information on the radial wave function $\Psi_{i[f]}(x,\mathbf{k}_\perp)$ (consequently $h_{1[2]}^{LF}$) can be obtained by LF CQM. The details of our variational procedure to determine both mass spectra and wave functions of pseudoscalar mesons were recently documented in [3, 4] along with an extensive test of the model in the spacelike exclusive processes. The same model is used in this work, that is, comparing the LF vertex functions Ψ in Eq. (12) with our light-front wave function given by [3, 4], we

[1]While one can in principle also consider the BS amplitude for Ψ_g, we note that such extension does not alter our results within our approximation in this work because both hadron and gauge boson should share the same kernel.

identify

$$\Psi(x,\mathbf{k}_\perp)=\left(\frac{8\pi^3}{N_c}\right)^{1/2}\left(\frac{\partial k_z}{\partial x}\right)^{1/2}\frac{[x(1-x)]^{1/2}}{M_0}\phi(x,\mathbf{k}_\perp), \tag{14}$$

where the Jacobian of the variable tranformation $\mathbf{k} = (k_z,\mathbf{k}_\perp)\to(x,\mathbf{k}_\perp)$ is obtained as $\partial k_z/\partial x = M_0/[4x(1-x)]$ and the radial wave function is given by

$$\phi(\mathbf{k}^2)=\left(\frac{1}{\pi^{3/2}\beta^3}\right)^{1/2}\exp(-\mathbf{k}^2/2\beta^2), \tag{15}$$

which is normalized as $\int d^3k|\phi(\mathbf{k}^2)|^2 = 1$. Substituting Eqs. (14) and (15) into Eqs. (10) and (11), one can obtain the valence and nonvalence contributions to the weak form factors for $0^-\to 0^-$ semileptonic decays in light-front quark model.

While the relevant operator $\mathcal{K}$ is in general dependent on all internal momenta $(x,\mathbf{k}_\perp,y,\mathbf{l}_\perp)$, a sort of average on $\mathcal{K}$ over y and $\mathbf{l}_\perp$ in Eq. (11) which we define as $G_{P_1P_2}\equiv\int[dy][d^2\mathbf{l}_\perp]\mathcal{K}(x,\mathbf{k}_\perp;y,\mathbf{l}_\perp)\Psi_f(y,\mathbf{l}_\perp)$ is dependent only on x and $\mathbf{k}_\perp$. Now, the range of the momentum fraction x depends on the external momenta for the embedded states. As shown in Eq. (11), the lower bound of x for the kernel in the nonvalence contribution is given by α which has the value $\alpha = M_2/M_1$ at the maximum q^2. As the mass difference between the primary and secondary mesons gets smaller, not only the range of q^2 is reduced but also α gets closer to 1. Perhaps, the best experimental process for such a limit may be the pion beta decay $\pi^\pm\to\pi^0e^\pm\bar\nu_e$, where our numerical prediction $f_-(0)/f_+(0) = -3.2\times10^{-3}$ following the treatment presented in this work is in an excellent agreement with -3.5×10^{-3} obtained by the method proposed by Jaus [14] including the zero-modes [8, 13, 15]. In Ademollo-Gatto's SU(3) limit [16], the q^2 range of the nonvalence contribution shrinks to zero and α becomes precisely 1. However, even if α is not so close to 1, the initial wavefunction $\Psi_i(x,\mathbf{k}_\perp)$ plays the role of a weighting factor in the nonvalence contribution and enfeeble the contribution from the region of x near 1. Thus, for the processes that we discuss in this talk, the effective x region for the nonvalence contribution is quite narrow. Similarly, the region of the transverse momentum $\mathbf{k}_\perp$ is also limited only up to the scale of hadron size due to the same weighting factor $\Psi_i(x,\mathbf{k}_\perp)$. Here, we thus approximate $G_{P_1P_2}$ as a constant and examine the validity of this approximation by checking the frame independence of our numerical results.

For the check of frame-independence, we also compute the "+" component of the current J_D^μ in the Drell-Yan-West ($q^+=0$) frame where only valence contribution exists. Since the form factor $f_+(q^2)$ obtained from J_D^+ in $q^+=0$ frame is immune to the zero-mode contribution [4, 8, 13, 14], the comparison of $f_+(q^2)$ in the two completely different frames (that is, $q^+=0$ and $q^+\neq0$) would reveal the validity of an existing model with respect to a covariance. The comparison of $f_-(q^2)$, however, cannot give a meaningful test of covariance because of the zero-mode complication as noted in [14]. Indeed, the difference between the two ($q^+=0$ and $q^+\neq0$) results of $f_-(q^2)$ amounts to the zero-mode contribution.

3. NUMERICAL RESULTS

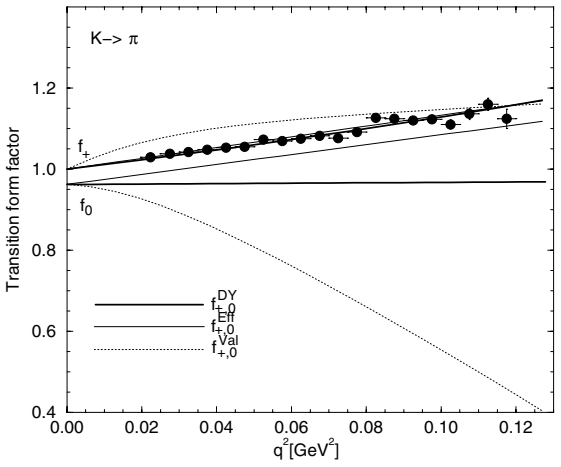

Figure 3: The weak form factors for $K^0_{\ell3}$ compared with the experimental data [17].

In our numerical calculation for the processes of $K_{\ell3}$ and $D^0\to K^-\ell^+\nu$ decays, we use the linear potential parameters presented in [4]. In Figure 3, we show the weak form factors $f_+(q^2)$ and $f_0(q^2)$ for $K^0_{\ell3}$ decays. The thick solid lines are our analytic solutions obtained from the $q^+=0$ frame; note here again that the lower thick solid line (f_0) in Figure 3 is only the partial result without including the zero-mode contribution while the upper thick solid line (f_+ immune to the zero-mode) is the full result. The thin solid lines are the full results of our effective calculations with a constant ($G_{K\pi}$=3.95) fixed by the normalization of f_+ at $q^2=0$ limit. For comparison, we also show only the valence contributions (dotted lines) in $q^+\neq0$ frame. As expected, a clearly distinguishable nonvalence contribution is found. Following the popular linear parametrization [18], we plot the results of our effective solutions (thin solid lines) using $f_i(q^2) = f_i(q^2 = m_\ell^2)(1+\lambda_i q^2/M^2_{\pi^+})(i=+,0)$. In comparison with the data, the same normalization as the data $f_+(0)=1$ [17] was used in Figure 3. Our effective solution (upper thin solid line) is not only in good agreement with the data [17] but also almost identical to that in $q^+=0$ frame(upper thick solid line) indicating the frame-independence of our model. Note also that the difference in $f_0(q^2)$ between $q^+\neq0$ (lower thin solid line) and $q^+=0$(lower thick solid line) frames amounts to the zero-mode contribution.

In comparison with experimental data, we summarized our results of several experimental observables in Table 1; i.e. the actual value of $f_+(0)$, the slopes λ_+ [λ_0] of $f_+(q^2)$ [$f_0(q^2)$] at $q^2=0$, $\xi_A = f_-(0)/f_+(0)$, and the decay rates $\Gamma(K^0_{e3})$ and $\Gamma(K^0_{\mu3})$. In the second column of Table 1, our full results including nonvalence contributions are presented along with the valence contributions in the square brackets. In the third column of Table 1, the results in $q^+=0$ frame are presented with [without] the instantaneous part. As one can see in Table

Table I Model predictions for the parameters of $K^0_{\ell 3}$ decays. The decay width is in units of 10^6 s^{-1}. The used CKM matrix is $|V_{us}| = 0.2196 \pm 0.0023$ [18].

	Effective	$q^+ = 0$	Experiment
$f_+(0)$	0.962 [0.962]	0.962 [0.962]	
λ_+	0.026 [0.083]	0.026 [0.026]	$0.0288 \pm 0.0015[K^0_{e3}]$
λ_0	0.025 [−0.017]	0.001 [−0.009]	$0.025 \pm 0.006[K^0_{\mu 3}]$
ξ_A	−0.013 [−1.10]	−0.29[−0.41]	$-0.11 \pm 0.09[K^0_{\mu 3}]$
$\Gamma(K^0_{e3})$	7.3 ± 0.15	7.3 ± 0.15	7.5±0.08
$\Gamma(K^0_{\mu 3})$	4.92 ± 0.10	4.66 ± 0.10	5.25±0.07

1, adding the nonvalence contributions clearly improves the results of λ_0, that is, our full result of $\lambda_0 = 0.025$ is in excellent agreement with the data, $\lambda_0^{\text{Exp.}} = 0.025 \pm 0.006$. Since the lepton mass is small except in the case of the τ lepton, one may safely neglect the lepton mass in the decay rate calculation of the heavy-to-heavy and heavy-to-light transitions. However, as one can see from the improved result for $K_{\mu 3}$ decay rate, the reliable calculation of $f_0(q^2)$ is required especially for $K_{\mu 3}$ since the muon(μ) mass is not negligible, even though the contribution of $f_0(q^2)$ is negligible for K_{e3} case.

In Figures 4(a,b), we show the weak form factors for $D^0 \to K^-\ell^+\nu$ decays and compare with the experimental data [18] (full dot) with an error bar at $Q^2 = 0$ as well as the lattice QCD results [19] (circle and square) and [20] (cross). All the line assignments are same as in Figure 3. In Figure 4(a), the thin solid line of our full result in $q^+ \neq 0$ is not visible because it exactly coincides with the thick solid line of the result in $q^+ = 0$ confirming the frame-independence of our calculations. Our value of $f_+(0) = 0.736$ is also within the error bar of the data [18], $f_+^{\text{Exp.}}(0) = 0.7 \pm 0.1$. In Figure 4(b), the difference between the thin and thick solid lines is the measure of the zero-mode contribution to $f_0(q^2)$ in $q^+ = 0$ frame. The form factors obtained from our effective calculations ($G_{DK} = 3.5$) are also plotted with the usual parametrization of pole dominance model, that is, $f_{+(0)}(q^2) = f_{+(0)}(0)/(1 - q^2/M^2_{1^-(0^+)})$. Our pole masses turn out to be $M_{1^-} = 2.16$ GeV and $M_{0^+} = 2.79$ GeV, respectively, and we note that $M_{1^-} = 2.16$ GeV is in good agreement with the mass of D_s^*, that is, 2.1 GeV. Using CKM matrix element $|V_{cs}| = 1.04 \pm 0.16$ [18], our branching ratios $\text{Br}(D^0_{e3}) = 3.73 \pm 1.24$ and $\text{Br}(D^0_{\mu 3}) = 3.60 \pm 1.19$ are also comparable with the experimental data 3.64 ± 0.18 and 3.22 ± 0.17 [18], respectively.

In Figure 5, we show the differential decay rates for $D^0 \to K^-e^+\nu_e$ and $D^0 \to K^-\mu^+\nu_\mu$ transitions obtained from our effective solutions. As in the case of $K_{\ell 3}$ decays, we were able to evaluate the $f_0(q^2)$ contribution to the total decay rate for $D^0 \to K^-\mu^+\nu_\mu$ process in a more reliable manner although its contribution is more suppressed than the $K_{\mu 3}$ case.

4. CONCLUSION

In summary, we presented an effective treatment of the LF nonvalence contributions crucial in the timelike exclusive processes. Using a SD-type approach and summing the LF time-ordered amplitudes, we obtained the nonvalence contributions in terms of ordinary LF wavefunctions of gauge boson and hadron that have been extensively tested in the spacelike exclusive processes. Including the nonvalence contribution, our results show a definite improvement in comparison with experimental data on $K_{\ell 3}$ and $D^0 \to K^-\ell^+\nu_\ell$ decays. Our result on π_{e3} is also consistent with the result obtained by other methods. Furthermore, the frame-independence of our results indicate that a constant $G_{P_1P_2}$ is an approximation appropriate to the small momentum transfer processes. A similar conclusion was drawn in a recent application of our method to the skewed quark distributions of the pion at small momentum transfer region [21]. Applications to the heavy-to-light decay processes involving large momentum transfers would require an improvement on this approximation perhaps guided by the perturbative QCD approach. Consideration along this line is underway.

Acknowledgements

The work of CRJ was supported in part by the US DOE under contracts DE-FG02-96ER40947 and that of HMC by the NSF grant PHY-00070888. The North Carolina Supercomputing Center and the National Energy Research Scientific Computer Center are also acknowledged for the grant of supercomputer time.

REFERENCES

[1] S. J. Brodsky, H.-C. Pauli, and S. S. Pinsky, Phys. Rept. **301**, 299(1998).
[2] W. Jaus, Phys. Rev. D **44**, 2851 (1991).
[3] H.-M. Choi and C.-R. Ji, Phys. Rev. D **59**, 074015 (1999); Phys. Rev. D **56**, 6010 (1997).
[4] H.-M. Choi and C.-R. Ji, Phys. Lett. B **460**, 461 (1999); Phys. Rev. D **59**, 034001 (1999).
[5] L. S. Kisslinger, H. -M. Choi, and C. -R. Ji, Phys. Rev. D **63**, 113005 (2001).

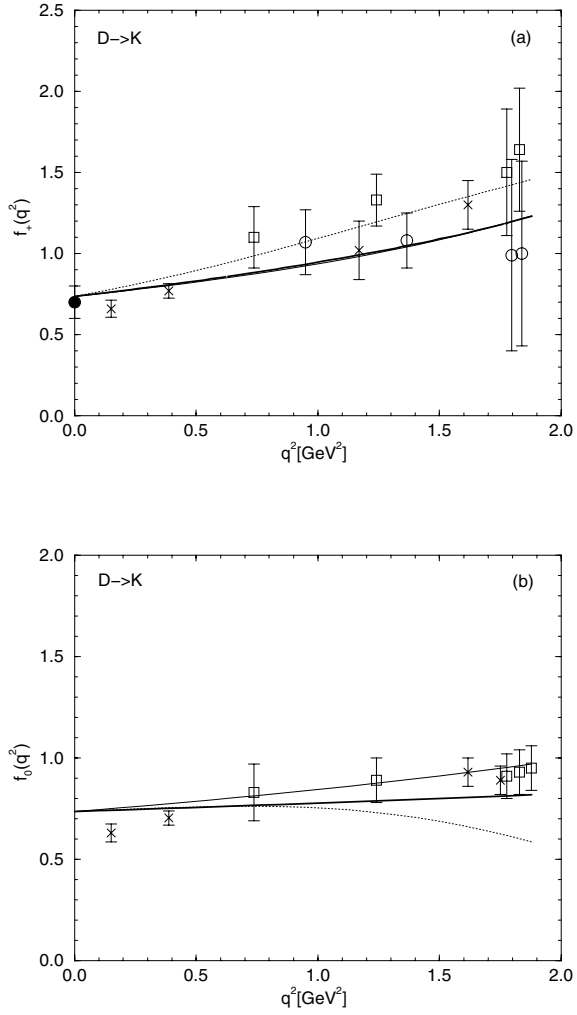

Figure 4: The weak form factors for $D \to K$ transition. The same line codes are used as in Figure 3.

[6] L. Susskind and M. Burkardt, pp. 5 in Proceedings of the 4th International Workshop on Light-Front Quantization and Non-Perturbative Dynamics edited by S. D. Glazek (1994); K. G. Wilson and D. G. Robertson, pp. 15 in the same proceedings.

[7] B. L. G. Bakker and C. -R. Ji, Phys. Rev. D **62**, 074014 (2000); B. L. G. Bakker, H. -M. Choi, and C. -R. Ji, Phys. Rev. D **63**, 074014 (2001).

[8] S. J. Brodsky and D. S. Hwang, Nucl. Phys. B **543**, 239 (1998).

[9] H.-M. Choi and C.-R. Ji, Nucl. Phys. A **679**, 735 (2001).

[10] C. -R. Ji and H. -M. Choi, to appear in Phys. Lett. B [hep-ph/0009281]; Nucl. Phys. B (Proc. Suppl.) **90**, 93 (2000).

[11] S.J. Brodsky, C.-R. Ji and M. Sawicki, Phys. Rev. D **32**, 1530 (1985); J.H.O. Sales, et. al., Phys. Rev. C **61**, 044003 (2000).

[12] M. B. Einhorn, Phys. Rev. D **14**, 3451 (1976).

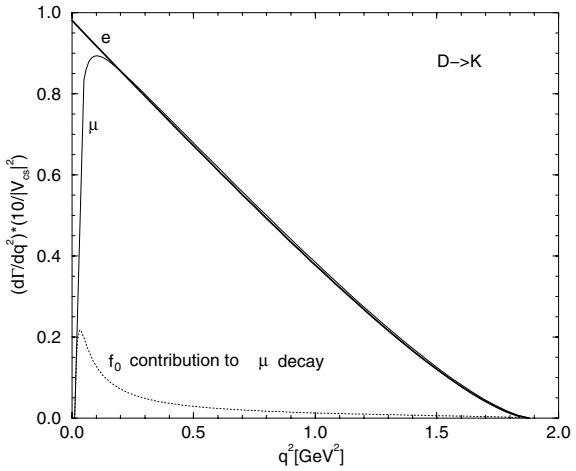

Figure 5: The differential decay rates for $D^0 \to K^-\ell^+\nu_\ell$ transition.

[13] H. -M. Choi and C. -R. Ji, Phys. Rev. D **58**, 071901 (1998).

[14] W. Jaus, Phys. Rev. D **60**, 054026 (1999).

[15] S. J. Chang, R. G. Root, and T. M. Yan, Phys. Rev. D **7**, 1133 (1973); T. M. Yan, *ibid*. **7** (1973) 1780; M. Burkardt, Nucl. Phys. A **504**, 762 (1989); Phys. Lett. B **268**, 419 (1991); N. E. Ligterink, B. L. G. Bakker, Phys. Rev. D **52**, 5917 (1995); *ibid*. **52**, 5954 (1995); N. C. J. Schoonderwoerd, B. L. G. Bakker, Phys. Rev. D **57**, 4965 (1998); J. P. B. C. de Melo et al., Nucl. Phys. A **660**, 219 (1999).

[16] M. Ademollo and R. Gatto, Phys. Rev. Lett. **13**, 264 (1964).

[17] Apostolakis A et al., Phys. Lett. B **473**, 186 (2000).

[18] Particle Data Group, Eur. Phys. J. C **3** (1998) 1.

[19] C. W. Bernard, A. X. El-Khadra, and A. Soni, Phys. Rev. D **43**, 2140 (1991).

[20] K. C. Bowler et al., Phys. Rev. D **51**, 4905 (1995).

[21] H. -M. Choi, C. -R. Ji, and L. S. Kisslinger, hep-ph/0104117.